ANNUAL SUMMARY REPORT

P10 Asphalt fatigue at Queensland temperatures: Year 2 progress report

Project No: 007177

Authors: Erik Denneman and Timothy Lam

Client: Queensland Department of Transport and Main Roads

Date: September 2015

AN INITIATIVE BY:

P10 ASPHALT FATIGUE AT QUEENSLAND TEMPERATURES: YEAR 2 PROGRESS REPORT

SUMMARY

Current pavement design approaches predict a shorter fatigue life for pavements in warm climates compared to those in colder climates. This is in contrast to field data, which indicates that pavements in warmer climates last longer before fatigue cracking occurs. There is a need to examine whether current pavement design models accurately reflect the nature of fatigue damage accumulation in thick asphalt pavements in Queensland. The development of improved models for predicting the fatigue life of asphalt pavements which better reflect operating conditions in Queensland could result in a significant reduction in the thickness of full depth asphalt pavements.

The object of Year 2 of the study was to characterise the fatigue performance of typical Queensland asphalt mixes at elevated temperatures. Laboratory experiments were performed on two Queensland asphalt base layer materials.

The findings of the study indicate that the fatigue performance of asphalt mixes can be successfully characterised using the new AGPT/T274 protocol up to temperatures of at least 30 °C.

The results confirm that the laboratory based fatigue prediction models in use in the current Austroads design method provide an acceptable prediction of fatigue performance. For other mixes there will be clear benefits in developing mix specific fatigue curves for use in pavement design.

A number of options for interim improvements to the asphalt pavement design methods used by TMR were listed in this study. Consultation with the Department will take place to discuss implementation. The introduction of the option to develop mix specific fatigue functions for the use in pavement design may be expected to drive three outcomes:

1. Optimisation of mixes in terms of balancing rut resistance, stiffness and fatigue performance
2. Encouragement of the use of innovative asphalt mix designs (e.g. EME2)
3. A significant reduction in pavement thicknesses.

CONTENTS

TABLES

FIGURES

1 INTRODUCTION

This progress report presents the findings from the second year of NACoE project P10: Asphalt fatigue at Queensland temperatures.

1.1 Background

Full depth asphalt pavement thicknesses in excess of 400 mm have been designed for heavily-trafficked urban road applications in Queensland. One of the reasons for the large thickness is that current pavement design models predict an increased rate of fatigue damage accumulation at high temperatures. This is a consequence of the higher strain levels generated in the pavement at elevated temperatures and the associated exponential reduction in asphalt modulus with temperature.

However, this negative correlation between pavement temperature and fatigue performance of pavements does not agree with field observations. Data from accelerated pavement testing (APT) studies overseas seems to indicate that, in contrast to what the current fatigue models predict, the majority of fatigue damage accumulation occurs at low temperatures rather than at elevated temperatures (Mateos et al. 2012; Pellinen et al. 2004; Stuart et al. 2002).

The issue is illustrated in Figure 1.1, which compares the predicted number of passes of the 80 kN Standard Axle load to fatigue failure ($N_{fatigue}$) with the weighted mean annual pavement temperature (WMAPT) for asphalt pavements of various thicknesses. The $N_{fatigue}$ values shown in the figure were calculated using the model in Part 2 of the Austroads Guide to Pavement Technology (AGPT) (Austroads 2012) assuming a subgrade modulus of 70 MPa and a full depth asphalt pavement. The asphalt moduli values were typical of size 14 asphalt with Class 320 bitumen at 25 °C presented in Table 6.13 of the AGPT adjusted for different temperatures using Figure 6.7 in the AGPT. According to the results in Figure 1.1 the pavement thickness in Brisbane (WMAPT of 32 °C) needs to be approximately 50 mm greater than a pavement in Melbourne (WMAPT of 24 °C) for the same design traffic loading.

Figure 1.1: Load repetitions to failure at different design temperatures

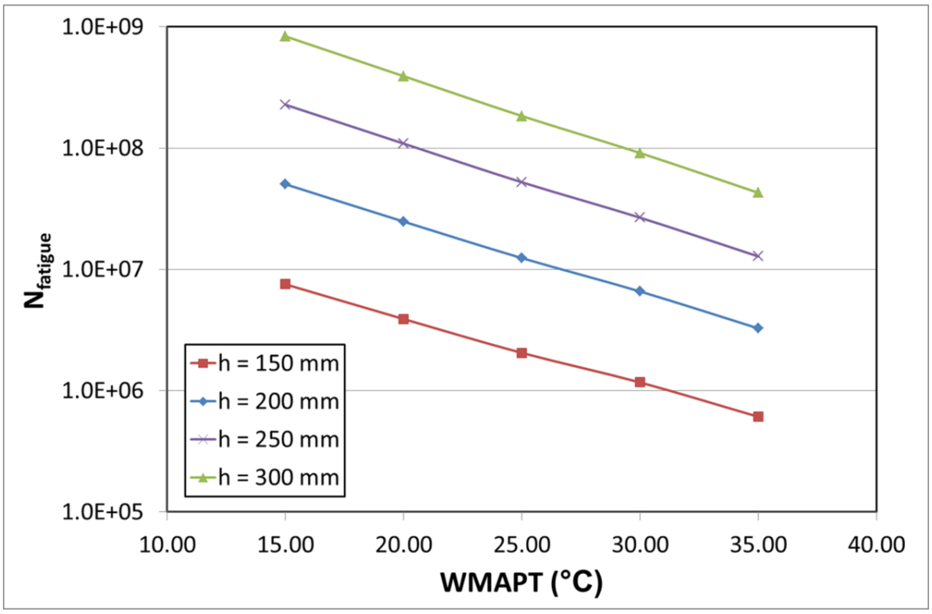

This NACoE project was established to address the discrepancy between predictive models and field performance and in doing so improve the cost-effectiveness of asphalt pavement design in Queensland.

1.2 Problem statement

There is a need to examine whether current pavement design models accurately reflect the nature of fatigue damage accumulation in thick asphalt pavements in Queensland. The development of improved models for predicting the fatigue life of asphalt pavements which better reflect operating conditions in Queensland could result in a significant reduction in the thickness of full depth asphalt pavements. There is also a need to improve the laboratory characterisation of asphalt fatigue at elevated temperatures. It may be necessary for Australia to play a leading role in this research, as fatigue prediction at elevated pavement temperatures is less of a priority in the USA and Europe.

1.3 Outcomes from Year 1 of the study

The literature survey performed as part of Year 1 of this study confirmed the need to improve the models for the prediction of fatigue in asphalt pavements at elevated temperatures (NACoE, forthcoming a). Current fatigue models predict the fastest accumulation of fatigue damage at higher temperatures, while available field data shows that most fatigue damage accumulates in cooler winter months. The analysis of a Federal Highway Administration (FHWA) Accelerated Loading Facility study also indicated that the current Austroads fatigue prediction model may be more conservative at elevated temperatures compared to low and medium temperatures.

The four-point bending test is the standard test for the characterisation of the fatigue performance of asphalt mixes in Australia. The literature review found that the four-point bending test is a suitable test method to characterise the fatigue behaviour of asphalt over a range of temperatures, although there were mixed reports on the suitability of the tests at temperatures over 30 ºC. No alternative method was identified that provides significant advantages over the four-point bending test. The proposed test program will therefore be based on four-point bending testing.

The literature review indicated that the low rate of fatigue damage accumulation in asphalt at high temperatures observed in the field and in the laboratory may be due to a number of factors, including slower crack growth due to lower stresses and stiffness and healing of the material. Healing is a function of the number and duration of rest periods, the viscosity of binder and temperature. The literature further indicated that there is at present no well-established method to characterise fatigue and healing properties based on binder testing only. The development of such a method would require a fundamental research program and it would be unlikely to yield results that would be implementable in the short to medium term.

1.4 Research hypothesis

Based on the work completed in Year 1 of this study it is expected that improvements to the models for the prediction of fatigue in asphalt pavements in Queensland can be achieved through the following steps:

1. Improving the characterisation of pavement temperature by adjusting the current definition of the WMAPT by correcting it for the variation of temperature with depth and investigating the use of a statistical temperature distribution in the pavement, rather than a single value.
2. Characterising the fatigue behaviour of typical Queensland mixes at different temperatures using four-point bending fatigue tests and using this data to develop temperature-dependent fatigue models for Queensland mixes.
3. Characterising the effect of rest periods on fatigue performance in laboratory tests and developing a temperature- and rest period-dependent component to the fatigue prediction models.
4. Investigating possible improvements to the shift function between laboratory and field fatigue performance.

1.5 Scope of study

It was expected that Step 1 of the above hypothesis will be addressed as part of a separate national research effort funded under the Austroads program. The design procedures for asphalt pavements in Queensland can be updated based on the outcomes of the Austroads program. It does therefore not form part of the scope for the present study, which will instead focus on addressing Steps 2, 3, and 4.

Laboratory experiments to address Steps 2 and 3 were started in Year 2, the laboratory experiments are due to be completed in Year 3. Step 4 will be addressed through a combination of interrogation of past pavement performance data and the construction of field experiments. The planning of field trials will commence in Year 3 of the study, with construction estimated to commence in Year 4. The field trials will be monitored over an extended period of time.

1.6 Objectives Year 2

In Year 2, the fatigue performance of typical Queensland asphalt mixes at elevated temperatures was characterised. The study also started to explore the effects of healing and rest periods and evidence of a fatigue endurance limit in the test.

The aim was to propose initial improved models for the prediction of fatigue in asphalt pavements in Queensland. An assessment was performed to evaluate to what extent these models will lead to reduced pavement thicknesses.

1.7 Structure of the report

This introductory section is followed by the presentation the results of experimental work completed in Section 2. Different fatigue models developed based on the experimental data are discussed in Section 3. Section 4 presents the updated experimental plan for Year 3. Options for interim implementation of the findings from the study are introduced in Section 5. Section 6 contains the conclusions and recommendations of the study.

2 EXPERIMENTAL WORK

The experimental work was performed in accordance with the experimental plan developed in Year 1 (NACoE forthcoming a). The work includes characterisation of modulus and fatigue performance for two Queensland asphalt base mixes, i.e. a DG20HM with Class 600 binder and an EME2 D14 mix design with 15/25 Penetration grade binder (EN 13924:2006). Both mixes had been part of a demonstration trial constructed at Cullen Avenue in Whinstanes as part of the EME2 technology transfer project. More information on the EME2 technology transfer effort performed as part of NACOE project P9 and Austroads project TT1908 can be found in Austroads (2014) and NACoE (forthcoming b). This section describes the fatigue characterisation of these mixes.

2.1 Mix design information

Both mixes were supplied from an asphalt plant in Whinstanes. The DG20HM mix is a TMR registered mix design complying with MRTS31 (April 2011, June 2013), mix registration number B:(I/C) DG20HM/13/981. The EME2 mix design was developed by the asphalt producer as part of the EME2 technology transfer effort and complies with the requirements in PSTS107 (May 2015). The mix design information is confidential and therefore cannot be disclosed in this report. However, the components of the DG20HM mix are contained in the TMR mix design register. For future reference, the EME mix composition can be defined as follows. The aggregates sources used for the EME2 mix design are the same as for the DG20. The proportions of the different aggregate fractions are 24.9% of 10/14 sized aggregate, 20.1% 6/10 sized aggregate, 6.8% 5/7 sized aggregate, 46.6% 0/4 sized aggregate and 1.6% baghouse fines. The EME2 mix contained 5.6% 15/25 penetration grade bitumen by mass of total mix.

2.2 Sample preparation

The asphalt material was mixed in the laboratory, from aggregate and binder sampled at the asphalt plant at the time of the construction of the Cullen Avenue trial. The laboratory prepared mix was used to create beam specimens in accordance with the procedures in AGPT/T220-2005. The specimens of the DG20HM were prepared to the conventional 5.0% ± 0.5% air voids. The specimens of the EME2 mix were prepared at 3.0% to 6.0% air voids (in accordance with the mix design requirements for EME2).

2.3 Modulus characterisation

The modulus (E*) of the material was characterised by means of flexural temperature/frequency sweep testing in accordance with the procedure in AGPT/T274-15. A set of four beams was tested. The average results obtained at each combination of temperature and frequency for the DG20HM mix are plotted in Figure 2.1. The full set of data for the DG20HM mix is provided in Table A 1 of Appendix A, with the results for the EME2 mix are provided in the report on NACoE project P9 (forthcoming). Also shown in Figure 2.1 is the master curve for the flexural modulus data. The master curve provides a convenient tool to determine the modulus at any combination of load frequency and temperature. The master curve is constructed by shifting the mean values obtained at the different frequencies for each temperature and frequency to form a continuous function at a reference temperature (T_i), in this case 20 ºC.

Figure 2.1: Temperature/frequency sweep data and master curve DG20HM

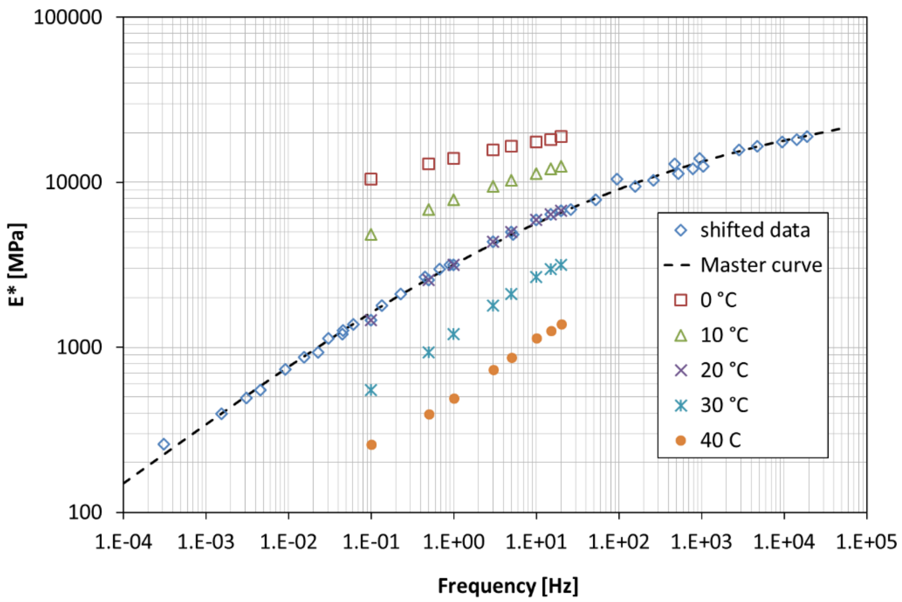

Derivation of the master curve is described in AGPT/T274-15. The master curve regression coefficients determined for the DG20HM and EME2 materials are shown in Table 2.1. The flexural modulus (E*) at any combination of temperature and frequency can be calculated using these regression coefficients in Equation 1, 2 and 3.

Table 2.1: Regression coefficients

Mix	δ	α	β	γ	a	b	c	R^2	Ti (°C)
DG20C600	0.1266	4.413	-1.181	-0.3404	0.0011	-0.1909	3.431	0.998	20
EME2	-5.794E-02	4.513	-1.839	-0.3151	3.754E-04	-0.1850	3.643	0.995	20

$$log|E^*| = \delta + \frac{\alpha}{1 + e^{\beta + \gamma \log f_r}} \quad 1$$

$$f_r = a(T) \times f \quad 2$$

$$\log a(T) = aT^2 + bT + c \quad 3$$

where

$\delta, \alpha, \beta, \gamma$ = fitting parameters

f = frequency (Hz)

f_r = reduced frequency (Hz)

$a(T)$ = shift factor as a function of temperature (°C)

T = temperature (°C)

a, b, c = fitting parameters

The E* master curves are shown in Figure 2.2. The shape of the curves indicates that the EME2 mix has a significantly higher modulus than the DG20HM at high temperatures and low load frequencies.

Figure 2.2: Master curve for DG20HM and EME2

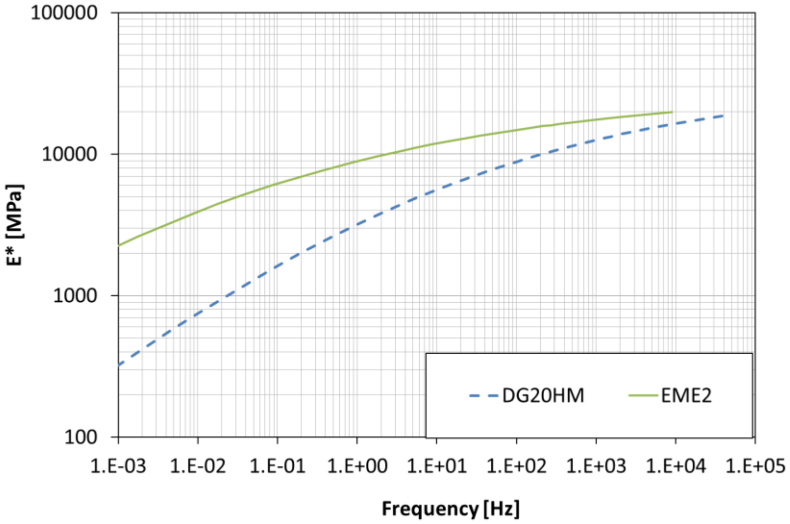

2.4 Fatigue testing

Four-point bending flexural fatigue testing was performed in accordance with AGPT/T274. The objective of the experiments was to characterise the fatigue behaviour of the EME2 and DG20HM mixes at different temperatures. Eighteen individual specimens were tested per temperature. Tests were undertaken divided over not less than three strain levels per temperature. The strain levels were chosen in such a way that the fatigue lives were within the range 10^4 to 2×10^6 cycles and the number of cycles to failure exceeded 10^6 for at least 20% of tests. All tests were performed at a load frequency of 10 Hz. The initial modulus was determined at the 50^{th} load cycle. In accordance with AGPT/T274, failure was defined as a 50% reduction in modulus. The number of sinusoidal displacement load cycles to reach this 50% reduction in modulus ($N_{f(50)}$) was reported. The results for individual specimens are shown in Table 2.2.

The DG20HM mix was tested at 10 °C, 20 °C, 30 °C and 40 °C. One of the aims of the testing on this initial mix was to investigate whether tests could be run successfully at higher temperatures than the conventional standard temperature of 20 °C. Analysis of the load response of the material during the tests showed that the test could be run successfully at 30 °C. The analysis of the results at 40 °C showed that the equipment was unable to impart a consistent sinusoidal loading to the specimens at this temperature. The effects are discussed in more detail in Section 2.5. It was therefore decided not to perform any further tests on asphalt mixes at this temperature. The EME2 mix was therefore tested at 10 °C, 20 °C and 30 °C.

The DG20HM mix was the first asphalt to be tested in the newly acquired flexural fatigue equipment at TMR. Teething problems during commissioning of the equipment led to considerable rework and as a consequence the bitumen sampled at the start of the project ran out. It was decided to sample a new batch of C600. Unfortunately, this change in binder led to an increase of approximately 30% in initial modulus across the various temperatures, linked with a far lower $N_{f(50)}$. The results for samples containing the second batch of C600 are highlighted in red in Table 2.2. It was decided to exclude these results from further analysis, as the change of binder clearly impacted fatigue performance.

Table 2.2: Fatigue results

DG20HM				EME2			
Sample #	Strain level (με)	$N_{f(50)}$	Temperature (°C)	Sample #	Strain level (με)	$N_{f(50)}$	Temperature (°C)
15-028-5	130	1,557,605	10	3355-3	160	859,148	10
15-029-1	130	1,615,599	10	3355-4	190	357,375	10
15-036-3	130	2,767,393	10	3356-1	220	134,693	10
15-007-1	180	264,377	10	3356-2	150	1,710,626	10
15-007-2	180	212,162	10	3362-3	230	37,320	10
15-007-3	180	143,807	10	3362-4	230	46,651	10
15-007-4	180	230,262	10	3399-3	230	129,239	10
15-007-5	180	230,262	10	3399-4	230	79,385	10
15-008-1	180	481,086	10	3400-2	230	21,616	10
15-008-2	280	13,646	10	3400-3	230	28,328	10
15-008-4	280	21,380	10	3401-1	220	64,489	10
15-008-5	280	23,714	10	3401-2	220	95,079	10
15-028-1	280	11,749	10	3401-3	220	34,903	10
15-110-4	130	180,281	10	3404-2	150	487,146	10
15-110-5	130	416,870	10	3404-3	150	164,755	10
15-113-3	130	172,487	10	3404-4	150	323,143	10
14-162-3	170	1,668,101	20	3415-1	115	1,307,976	10
14-162-4	170	959,892	20	3421-3	115	1,394,343	10
14-187-3	170	1,107,757	20	3415-3	115	3,577,000	10
14-105-3	200	420,990	20	3421-4	115	1,174,642	10
14-105-4	200	215,504	20	3129-1	200	40,880	20
14-105-5	200	269,188	20	3129-2	200	135,660	20
15-065-4	200	457,089	20	3129-3	200	256,000	20
14-140-2	300	30,695	20	3129-4	200	136,720	20
14-140-5	300	140,611	20	3129-5	200	475,910	20
14-148-1	300	79,403	20	3129-6	200	71,360	20
15-033-1	300	23,805	20	3130-1	160	900,690	20
15-033-2	300	41,052	20	3130-2	160	1,465,630	20
15-036-1	300	50,312	20	3130-3	160	1,370,630	20
15-092-3	170	255,075	20	3130-4	160	2,267,010	20
15-092-4	170	232,631	20	3130-5	160	1,777,340	20
15-092-5	170	197,495	20	3130-6	160	1,323,870	20
15-109-2	170	116,592	20	3131-1	185	412,430	20
15-109-3	170	170,260	20	3131-2	185	386,260	20
15-092-1	200	73,283	20	3131-3	185	411,760	20
15-092-2	200	17,512	20	3131-4	185	387,880	20
14-189-5	240	1,605,298	30	3131-5	185	886,560	20
14-190-1	240	1,188,503	30	3131-6	185	545,550	20

DG20HM				EME2			
14-190-2	240	1,168,504	30	3315_2	300	181,450	30
14-188-2	400	100,000	30	3315_3	380	39,514	30
14-189-2	400	67,609	30	3315_4	380	39,528	30
14-189-4	400	74,703	30	3329-2	380	26,901	30
15-064-5	400	61,660	30	3329-3	380	36,012	30
15-065-1	400	50,895	30	3329-4	380	29,903	30
15-065-2	400	30,084	30	3339-1	380	36,550	30
14-188-4	475	32,360	30	3339-2	300	145,685	30
14-188-5	475	36,308	30	3339-3	300	170,103	30
14-189-1	475	31,142	30	3339-4	300	175,642	30
15-032-2	475	26,710	30	3342-1	300	125,657	30
15-032-4	475	13,751	30	3342-2	300	146,121	30
15-032-5	475	22,131	30	3342-3	215	3,542,192	30
15-109-4	240	274,018	30	3355-1	215	2,450,110	30
15-109-5	240	190,547	30	3355-2	230	1,126,439	30
15-110-1	240	113,067	30	3359-3	230	1,255,172	30
15-036-4	300	1,267,004	40	3361-2	230	2,570,519	30
15-051-2	300	1,086,704	40	3399-1	230	2,794,252	30
15-051-3	300	1,129,218	40	3400-1	230	903,692	30
15-052-2	300	698,948	40	3405-4	230	1,789,321	30
15-052-4	300	1,143,756	40				
15-064-3	300	1,564,749	40				
14-219-1	475	271,228	40				
14-219-3	475	74,132	40				
14-219-4	475	81,284	40				
15-063-1	475	98,100	40				
15-063-2	475	45,709	40				
15-064-1	475	163,431	40				
15-005-3	550	42,658	40				
15-005-5	550	99,236	40				
15-006-2	550	155,279	40				
15-029-2	550	50,700	40				
15-029-3	550	43,820	40				
15-029-5	550	69,717	40				

The fatigue results for the DG20HM and EME2 mixes are plotted in Figure 2.3 and Figure 2.4 respectively. The effect of temperature on fatigue performance is clearly visible in the figures. Also shown in the figures are the log-linear regression lines fitted to the data at each temperature. The regression procedure is discussed in Section 3. The EME2 data at 10 °C shows considerable scatter, more than would typically be expected for fatigue results. This may in part be due to the range in voids in the beam specimens (3.0%-6.0%, which complies with EME2 specifications) and possibly due to the brittle nature of the material at this low temperature.

Figure 2.3: DG20HM fatigue results at different temperatures

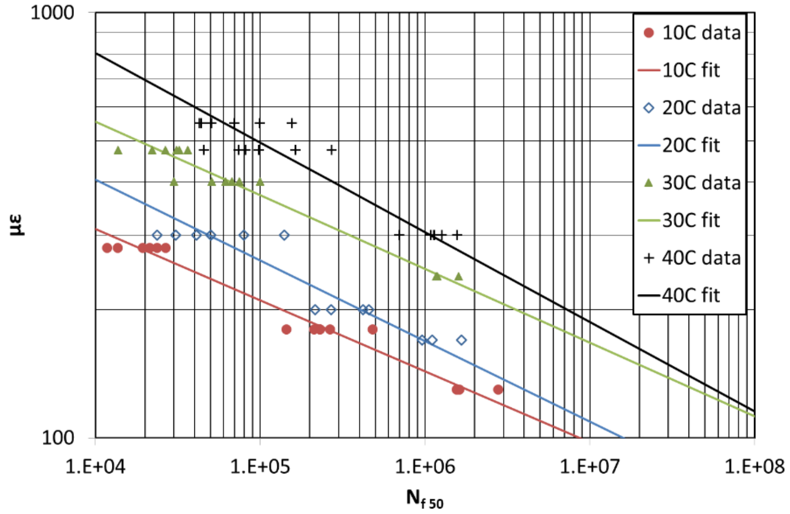

Figure 2.4: EME2 fatigue results at different temperatures

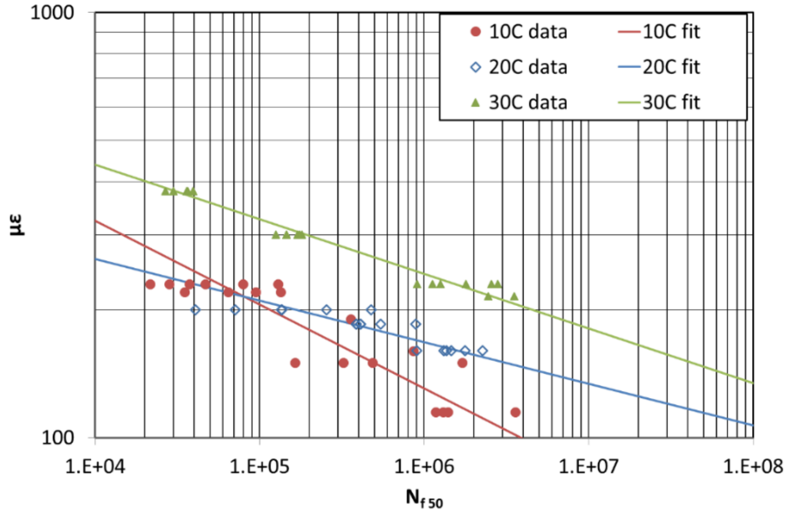

2.5 Fatigue data compliance at elevated temperatures

It has been reported previously that there are considerable practical challenges in characterising fatigue at temperatures above 30 °C using the four-point bending test configuration (Tsai 2003). One of the aims of the experimental work on the first mix was to assess whether it was possible to perform reliable fatigue tests at higher temperatures. At high temperatures, the modulus of the asphalt material reduces and it becomes increasingly viscous. This represents a challenge in achieving an acceptable sinusoidal displacement-load response during the test. Displacement-load response curves for randomly selected results for tests on DG20HM specimens run at the lowest strain level for each temperature are shown in Figure 2.5. Displacement-load curves are shown for the 50th, the 100,000th and the 1,000,000th cycle. The data shows that at 40 °C the equipment did not manage to induce a well-controlled sinusoidal displacement and load response in the sample. This can be observed in the unsmooth nature of the displacement loops shown in Figure 2.5d. Therefore, the reliability of the data at this temperature has to be questioned. Based on these results and the findings of the earlier work by Tsai (2003), it was decided to use 30 °C as the maximum temperature to run the test at for further mixes.

Figure 2.5: Load-displacement curves at: a) 10 °C, b) 20 °C, c) 30 °C and d) 40 °C

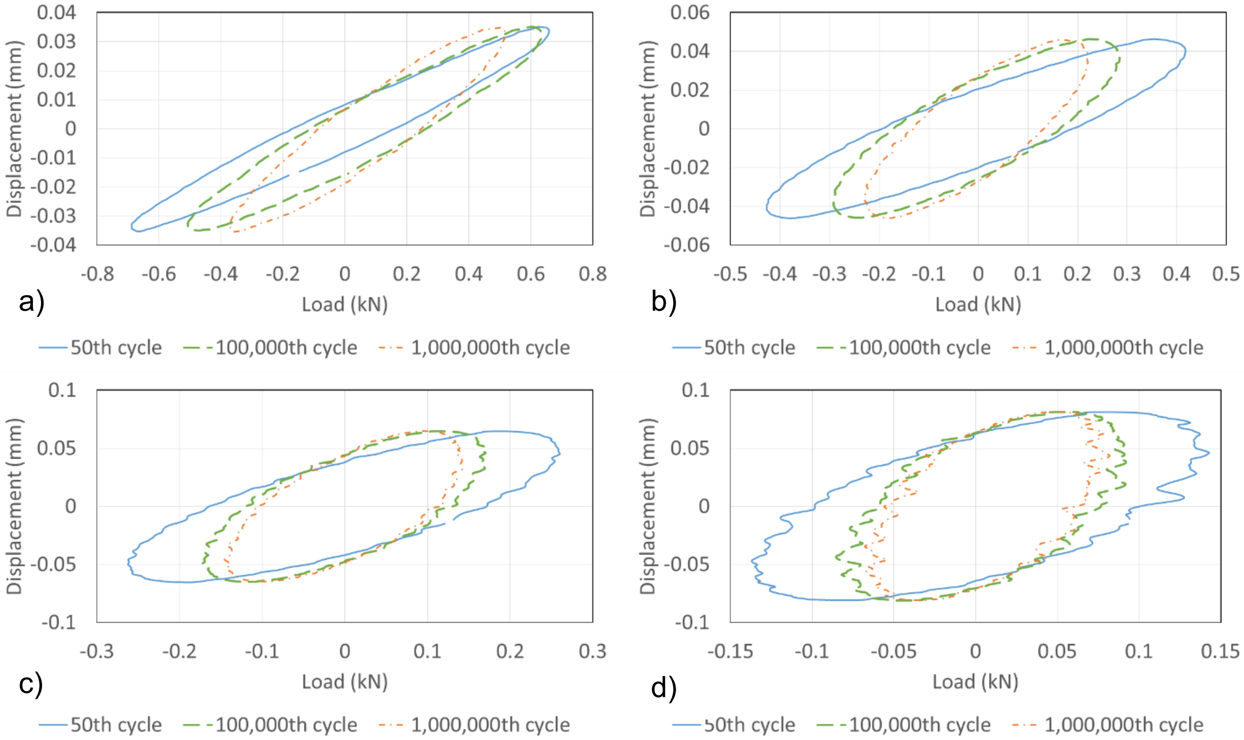

2.6 Exploring the effects of healing and rest periods

The concept of healing taking place in asphalt between load cycles is not new, having been reported since at least the late 1960s, e.g. Bazin and Saunier (1967); Van Dijk and Visser (1977). It is also mentioned in the Shell Pavement Design Method (Shell 1978). These publications have discussed how rest periods between load applications resulted in longer fatigue lives. Rest periods in fatigue tests have recently been applied in an extensive study on fatigue endurance limits by Witczak et al. (2013). The research claimed success in estimating the endurance limit from beam fatigue and uniaxial fatigue tests. Based plots of the stiffness ratio (SR) versus number of load cycles, the endurance limit was determined graphically for specimens with different initial asphalt mix stiffness (E_o) and rest periods. The SR is defined as the ratio between the measured stiffness at any point during the test and the initial stiffness. A typical plot of SR vs log (N) is shown in Figure 2.6. It is noted that, in order to reduce the testing time for test with rest period, sensitivity analysis was conducted to confirm that it is adequate to use the first 20 000 cycles to extrapolate up to 200 000 cycles.

Figure 2.6: Typical extrapolation to estimate SR (with rest period).

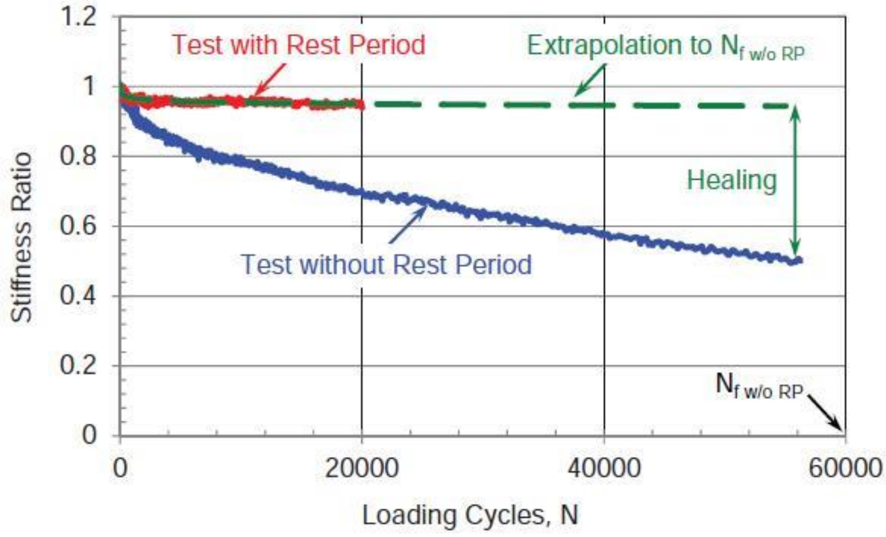

Since healing is expected to have a significant influence on fatigue performance, especially at elevated temperatures, it will be investigated as part of the experimental work under this project. An initial explorative experiment with healing was performed in Year 2. Comparative testing with and without rest period was performed on the EME2 material. The test was run at a low strain level of 100 micro strain, 10Hz at 20 °C. In the test with rest period, each sinusoidal load pulse was followed by a 1 second rest period. The intention was to run the test with rest period for as long as possible, during the closure of the ARRB laboratory over the Christmas break. Unfortunately, the computer ran out of memory after 84,000 cycles, therefore only this part of the test was recorded.

The result is plotted in Figure 2.7. The subsequent test without rest period was therefore programmed to run up to 100,000 cycles. The figure clearly shows the difference in modulus change during the test. The test without rest period shows a gradual decrease in modulus. The test with rest period unexpectedly shows an increase in modulus, the reason why this happened is not directly clear. After the initial increase, the modulus plateaus out and possibly starts to show a slight reduction with further loading. What is clear from this initial explorative testing is that rest periods significantly influence fatigue performance and a proposed plan for further experiments is presented in Section 4.

Figure 2.7: Result of fatigue test on EME2 mix with and without 1s rest period

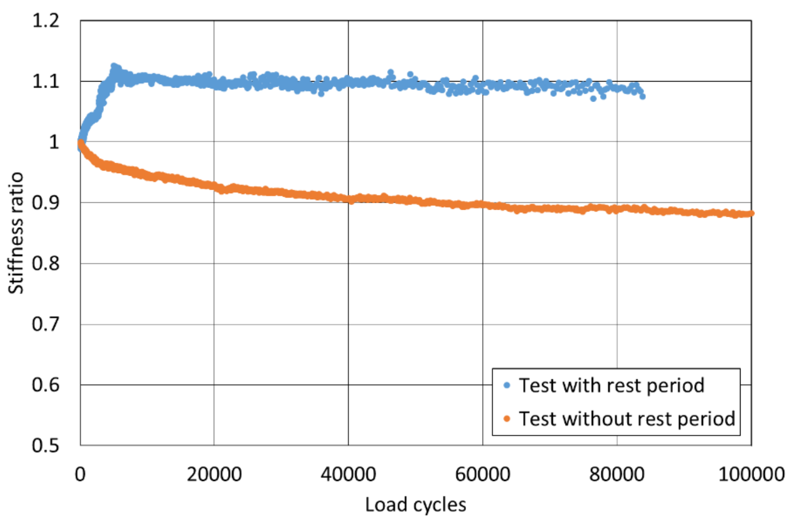

3 FATIGUE MODELS

The fatigue behaviour of the asphalt samples in the laboratory tests can be described using a variety of different models. A log-linear model is often used to describe the fatigue performance of asphalt as a function of strain level at a single temperature and load frequency. Log-linear regression of the fatigue data produced as part of this study will be presented in Section 3.1. By introducing the modulus (E*) of the material as a variable to the regression analysis in addition to the strain level it becomes possible to create a model that is temperature dependent. A temperature dependent model is fitted to the data in Section 3.2. The literature review in Year 1 of this study identified this software as of particular interest because it contains a loading time, temperature and rest period dependent shift factor for fatigue.

3.1 Log-linear regression

The relationship between the experimental stress or strain level and the cycles to fatigue failure (N_f) of asphalt (as well as fatigue for other materials such as metals or concrete) can be suitably represented using a linear function. The log of $N_{f(50)}$ is plotted against the stress or strain level, or alternatively the log of the stress or strain level. In this report the natural logarithm is used for the linear regression (in accordance with AGPT/T274), taking the form as shown in Equation 4. An example of this linear model is shown in Figure 3.1 for the results of testing on the EME2 mix at 30 °C.

$$\ln(N_{f(50)}) = a + b\ln(\varepsilon_{\mu}) \tag{4}$$

where

$N_{f(50)}$ = number of cycles to 50% stiffness reduction

a, b = constants determined from a set of fatigue test results

ε_{μ} = strain in μm/m (micro strain)

Figure 3.1: Mean fatigue curve EME2 data at 30 °C

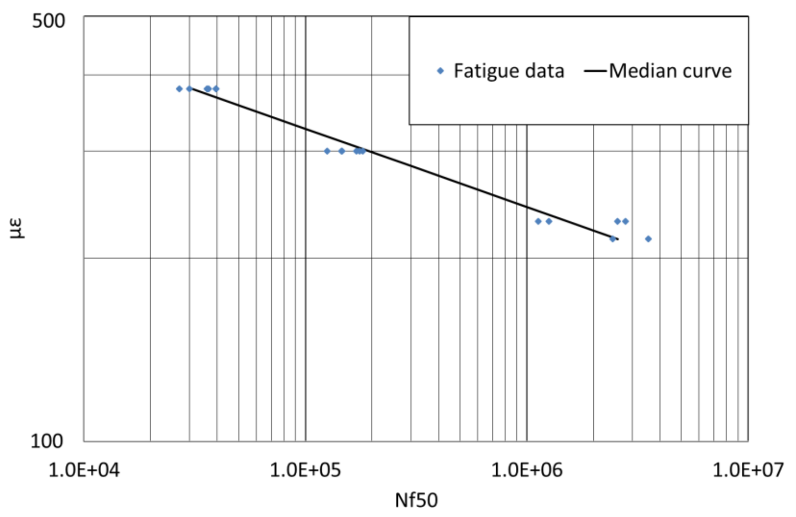

It has become convention, to plot log (N_f) on the horizontal axis and log (εμ) on the vertical axis as shown in Figure 3.1. Despite this method of visualisation, for the statistical analysis, strain is taken as the independent variable X and N_f as the dependent variable Y.

To fit Equation 1 to the data, we define Y = ln ($N_{f(50)}$) and X = ln (εμ) and therefore rewrite Equation 1 as Y=a+bX. The linear fit of the model to data may be obtained using a least-squares curve fit function available in spreadsheet software. Alternatively, the regression coefficients *a* and *b* may be determined as follows:

$$a = \bar{Y} - b\bar{X} \tag{5}$$

and

$$b = \frac{\sum_{i=1}^{n}(X_i - \bar{X})(Y_i - \bar{Y})}{\sum_{i=1}^{n}(X_i - \bar{X})^2} \tag{6}$$

where

$\bar{Y}$ = Mean Y value of test data

$\bar{X}$ = Mean X value of test data

The residuals R_i for the fitted data are determined using:

$$R_i = Y_i - \hat{Y}_i \tag{7}$$

$$\hat{Y}_i = a + bX_i \tag{8}$$

where

$\hat{Y}_i$ = Predicted value of Y

The standard deviation σ_y of the residuals is calculated from:

$$\sigma_y = \left(\frac{(Y_i - \hat{Y}_i)^2}{n-2}\right)^{\frac{1}{2}} \tag{9}$$

where

n = Number of samples

The significance of σ_y is that it allows the determination of confidence limits for the prediction of ln($N_{f(50)}$) and regression parameters a and b.

3.1.1 Confidence interval for $N_{f(50)}$

Using σ_y it is possible to determine with a confidence of (1- *α*) that a proportion *γ* of future samples tested will have a $N_{f(50)}$ exceeding a certain minimum value. Figure 3.2 shows the confidence interval corresponding to significance level α = 5%, probability *γ* = 95% for the EME2 fatigue data at 30 °C. In other words, there is 95% confidence in the prediction that 95% of future fatigue measurements on this material will yield a result to the right of the 95/95 confidence interval. The confidence interval is calculated from:

$$Y = a + bX - c_{(1-\alpha),\gamma}\sigma_y \qquad 10$$

where

$c_{(1-\alpha),\gamma}$ = Multiplier for one-sided tolerance limit

Figure 3.2: Fatigue results with confidence band for mean and 95/95 tolerance limit

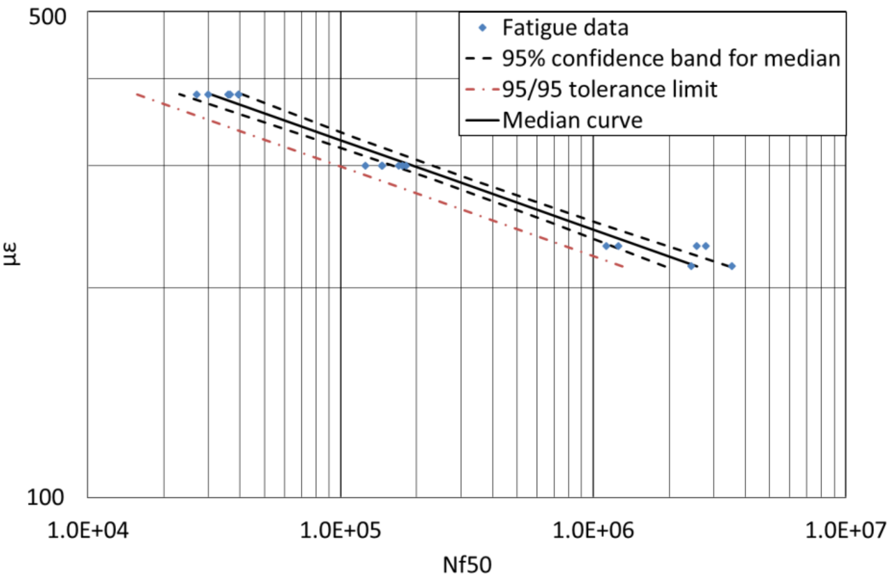

The value of $c_{(1-\alpha),\gamma}$ is a function of α, γ and n. It can be found in statistical tables. For this study the values available in the open source statistical software *R* were used. For typical fatigue studies n = 18, α = 0.05 and γ = 0.95, the value of $c_{(1-\alpha),\gamma}$ is 2.45.

It now possible to plot the confidence limits or different levels of reliability as shown in Figure 3.3.

Figure 3.3: Various levels of confidence in fatigue results for EME2 mix at 30 °C

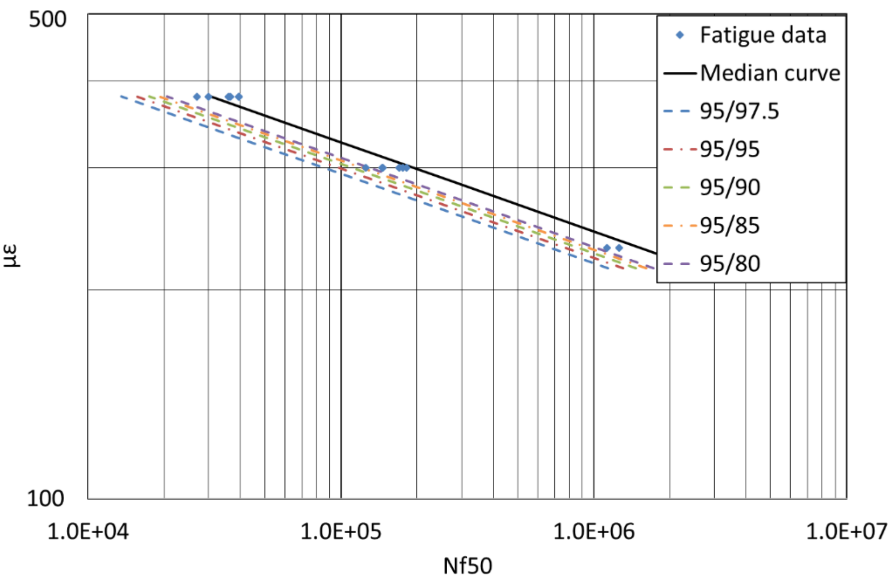

3.1.2 Confidence band for the mean curve

The exact position of the fatigue curve is unknown. The mean fatigue curve is a best estimate based on a limited number of observations. Regression parameters for the position and slope of the mean fatigue curve, i.e. intercept (*a*) and slope (*b*) can vary within a certain confidence band. The confidence band for the mean line can be calculated using Equation 11.

$$a + bX \pm \sqrt{2F_p}\,\sigma_y \left(\frac{1}{n} + \frac{(X_i - \bar{X})^2}{\sum_{i=1}^{n}(X_i - \bar{X})^2}\right)^{1/2} \quad 11$$

where

F_P = critical F-value for dataset

Using this approach, the confidence band for the mean can be plotted. The F value for 95% confidence, 18 specimens and 2 degrees of freedom (a and b) is 3.63. Using this approach the designer can be 95% confident that the true mean line of Y=a+bX will fit within the hyperbolic confidence limits drawn in Figure 3.2.

3.1.3 Linear regression coefficients for fatigue results from the study

The linear regression analysis was performed on the successful tests listed in Table 2.2. This excludes the DG20HM samples containing the second batch of binder and the results for tests performed at 40 °C for reasons discussed in Section 2.5. The regression parameters at different temperatures are shown in Table 3.1. These parameters are sufficient input to plot the mean fatigue curve, the different levels of confidence tolerances for the fatigue results and the confidence band for the mean curve. The results of the log-linear regression analysis at 95% confidence tolerance limits are plotted in Figures A.1 to A.6 of Appendix A. The results clearly show the influence of the number of successful tests *n* and the scatter around the mean curve σ_y on the width of the confidence interval limits.

Table 3.1: Linear regression parameters

Mix	Temperature	n	a	b	σ_y
DG20HM	10 °C	15	43.52	-5.983	0.343
DG20HM	20 °C	13	40.87	-5.274	0.523
DG20HM	30 °C	15	45.70	-5.777	0.349
EME2	10 °C	20	38.54	-5.074	0.697
EME2	20 °C	18	44.89	-5.574	0.558
EME2	30 °C	18	56.54	-7.780	0.311

3.1.4 Comparison of linear regression results with Shell laboratory fatigue model

The fatigue model in the current Austroads Guide is based on the fatigue relationship in the Shell Pavement Design Manual (SPDM) (Shell 1978). The Shell models represent the oldest and most widely used method for prediction of the fatigue resistance of asphalt pavements (Pellinen et al. 2004). The SPDM fatigue equation was developed based on results of two and three point, sinusoidal, displacement controlled, bending tests on thirteen mixes, as published by Van Dijk and Visser (1977).

The SPDM relationship for fatigue performance of asphalt in laboratory tests is shown in Equation 12. In the SPDM, the proposed use of this equation was to calculate the permissible strain in the asphalt (ε_{fat}) with a given binder content (V_b) [%] and mix stiffness (S_{mix}) [N/m^2] to yield a number of fatigue cycles (N_{fat}) to failure:

$$\varepsilon_{fat} = (0.856 \cdot V_b + 1.08) S_{mix}^{-0.36} \cdot N_{fat}^{-0.2} \qquad 12$$

The predictive model for fatigue damage to asphalt as currently contained in the Austroads Guide to Pavement Technology is shown as Equation 13. The SPDM equation is used in rewritten form to yield the number of allowable load repetitions (N) as a function of the volume of binder (V_b) [%] in the asphalt mix, the flexural modulus (E) [MPa] of the asphalt and the tensile strain ($\mu\varepsilon$), in microstrain, at the bottom of the asphalt layer:

$$N = RF \left[\frac{6918\,(0.856\, V_b + 1.08)}{E^{0.36} \mu\varepsilon} \right]^5 \qquad 13$$

A reliability factor (RF) is used in the Austroads Guide to relate laboratory fatigue life results to desired level of prediction of the in-service fatigue life. The RF value incorporates a shift factor for the differences between laboratory test conditions and field conditions as well a design reliability factor. The SPDM also indicated the need to use a shift function to translate the results of the laboratory model to field conditions. For the development of the design charts in the 1978 version of the SPDM, shift factors ranging from 5 to 28 were used to relate the predictions of the laboratory model in Equation 12 to field performance (Gerritsen and Koole 1987, Shell 1998).

Figure 3.4 and Figure 3.5 show the relative fatigue performance of the mixes tested in this study compared to the performance predicted by the Shell laboratory model in Equation 12. The input parameters for the Shell prediction relevant to these mixes are provided in Table 3.2. The results indicate that for some mixes there is a benefit in developing a mix specific fatigue equation. Laboratory testing can be used to show that some mixes outperform the default Shell fatigue prediction model. At higher temperatures, the slope of the fatigue line may be expected to change as well, leading to prediction of a higher number of load applications to failure at low strain levels.

Importantly, the use of mix specific fatigue curves instead of the standard Shell laboratory model will encourage optimisation of mixes for fatigue performance and innovative mix designs.

Figure 3.4: Comparison experimental mean curves from experimental data and Shell prediction model DG20HM

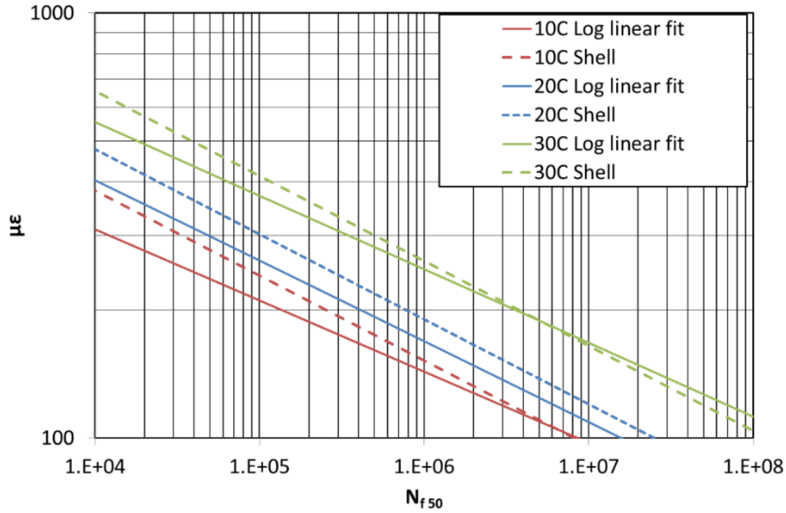

Figure 3.5: Comparison experimental mean curves from experimental data and Shell prediction model EME2

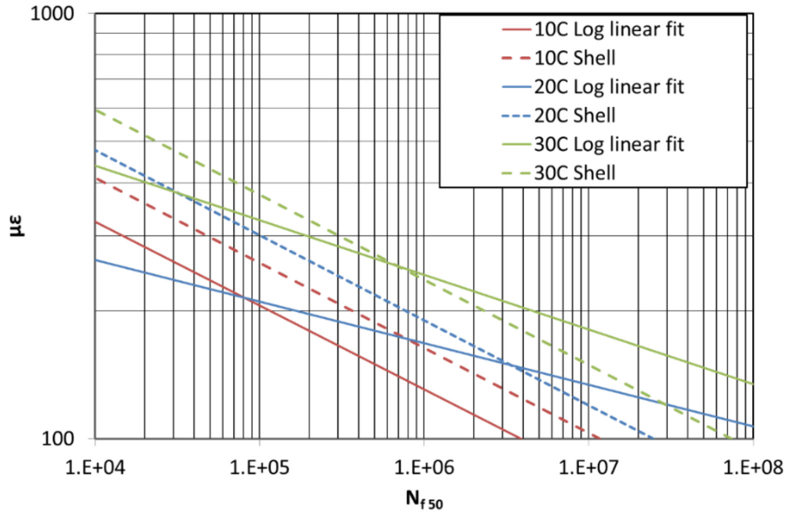

Table 3.2: Input parameters for the Shell laboratory model

Mix	DG20HM	EME2
Maximum density mix (kg/m^3)	2548	2339
Density Bitumen (kg/m^3)	1030	1030
Air void content (%)	5.0	5.0
Binder content by mass (%)	4.7	5.6
Volume of binder (V_b) (%)	11.0	12.7

3.2 Temperature dependent model

A major advantage of the Shell laboratory Equation 12 is that it includes the flexural modulus E as a variable and therefore can be used to predict fatigue performance at any combination of loading time and temperature. In contrast the linear regression model discussed in the previous section is developed for a single temperature and loading time which limits its application.

It is possible to fit a modulus (and therefore temperature and loading time) dependent fatigue model to the data obtained in this study. The model form shown as Equation 14 can be used for this purpose (CROW 2010).

$$\ln(N_f) = c_1 \cdot ln^3(E) + c_2 \cdot ln^2(E) + c_3 \cdot \ln(E) + c_4 + c_5 \cdot \ln(\epsilon) \quad 14$$

where

N_f = Number of load cycles to 50% reduction in modulus

E = Modulus of the asphalt (MPa)

ε = strain in µm/m

c_1-c_5 = regression coefficients

The model in Equation 14 can be fitted to fatigue data obtained at different temperatures and/or load frequencies. Figure 3.6 and Figure 3.7 show this temperature dependent model fitted to the fatigue data for the DG20HM and EME2 mixes respectively. The model was fitted using the Microsoft Excel solver function by maximising the coefficient of determination R^2 of the fit. The regression parameters for the best fit to data are shown in Table 3.3. A feature of this model is that the intercept of the fatigue equation is a function of E, while the slope of the fatigue curve (c_5) is independent of E and therefore constant for all temperatures. The dashed lines in the figures below are therefore all parallel.

Figure 3.6: Comparison linear model and temperature dependent model DG20HM

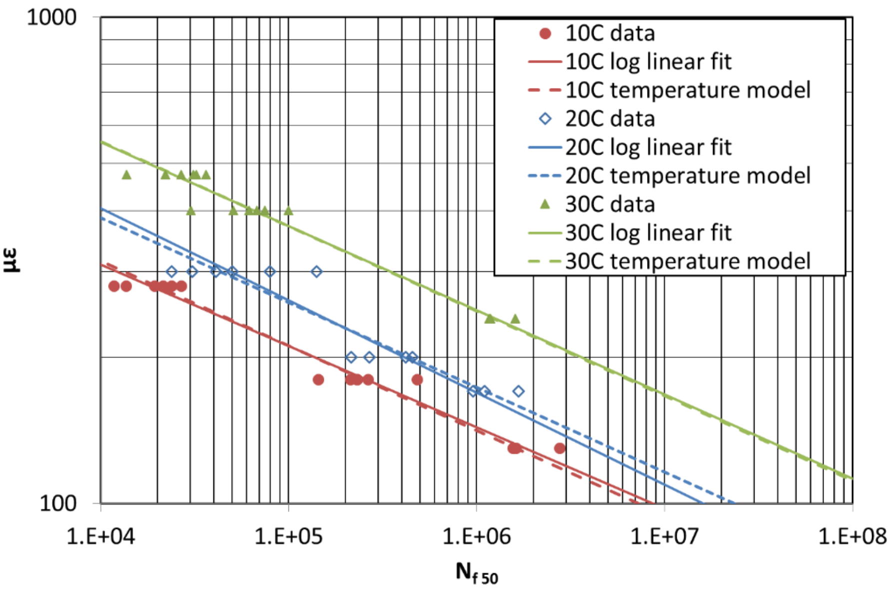

Figure 3.7: Comparison linear model and temperature dependent model EME2

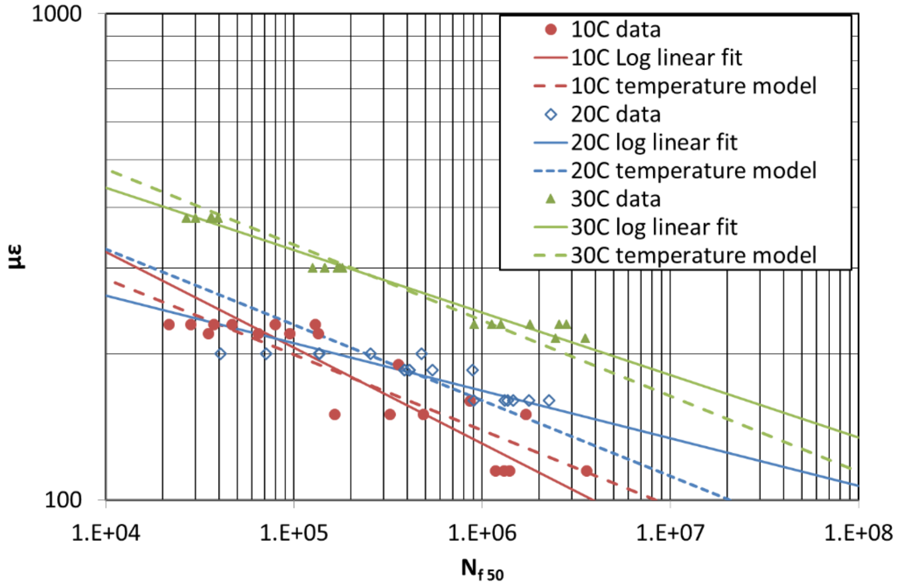

Table 3.3: Regression parameters for the temperature dependent fatigue model

Mix	n	c_1	c_2	c_3	c_4	c_5	σ_y
DG20HM	43	0.4076	-10.31	84.43	-179.4	-5.705	0.3955
EME2	58	0.4878	-11.61	86.66	-148.1	-6.430	0.6366

It is possible to plot one-sided tolerance for this fatigue fit as well. The 95/95 tolerances for the DG20HM temperature dependent fatigue curve at different temperatures is plotted in Figure 3.8.

Figure 3.8: Temperature model with 95/95 one-sided tolerance limit

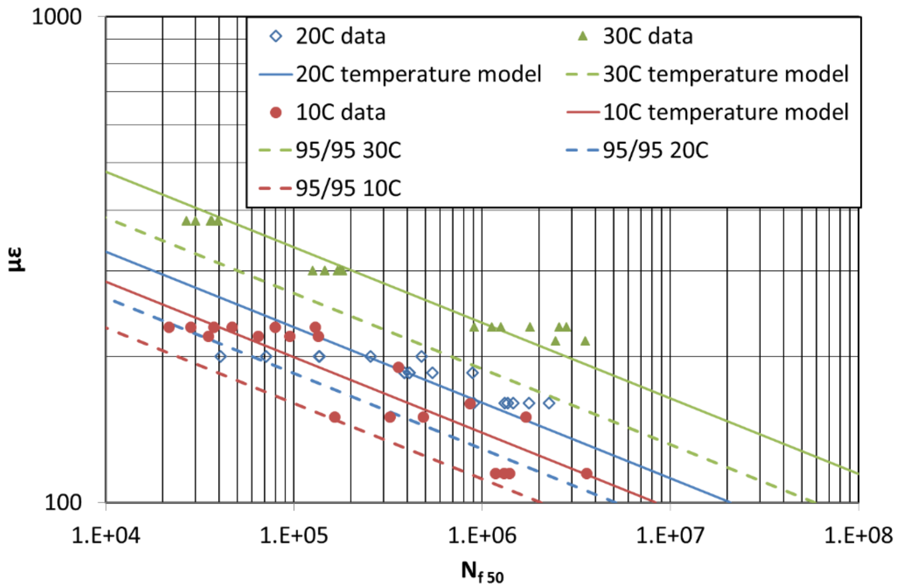

4 UPDATED EXPERIMENTAL PLAN

Based on the findings of Year 2 of the study, a number of changes to the experimental plan are proposed. The proposed changes affect the number of fatigue specimens to be tested per temperature condition and the loading mode for the rest period testing.

4.1 Temperature related fatigue tests

In Year 2 of the study, the intent was to test 18 beams per temperature for each mix. This is based on the well-established best practice of using a minimum of 18 beams to fit a linear fatigue curve. It has been shown that 18 specimens are required to ensure a sufficient level of confidence in the results.

However, if the aim is to fit a temperature dependent model such as shown in Equation 14, then it may be possible to reduce the number of specimens tested at each temperature, while still achieving a statistically acceptable fit, since a regression line with a fixed slope is fitted to the combined data points at different temperatures. To investigate the effect of sample size on the fit of the temperature dependent model, the datasets in Table 2.2 were reduced by eliminating data points. For each strain level the data points were eliminated, starting from the bottom, such that a set of 27 data points (3 specimens per strain level, 9 specimens per temperature), and a set of 18 data points (2 specimens per strain level, 6 specimens per temperature) were created. The resulting regression lines are shown in Figure 4.1 for the DG20HM mix and in Figure 4.2 for the EME2 mix. The regression parameters are provided in Table 4.1. The reduction in sample size has limited effect on the regression curve for the DG20HM mix. The fit for the EME2 mix is affected to a higher degree. This is mainly due to the scatter in the EME2 fatigue data at 10 °C.

Statistically, the confidence in the fit of the temperature dependent model based on testing at three temperatures, with three strain levels per temperature and two beams per strain level (18 specimens in total), is equivalent to the confidence for the linear fit to a set of 18 specimens tested at a single temperature.

Figure 4.1: Fit of temperature dependent model to DG20HM data based on different sample sizes

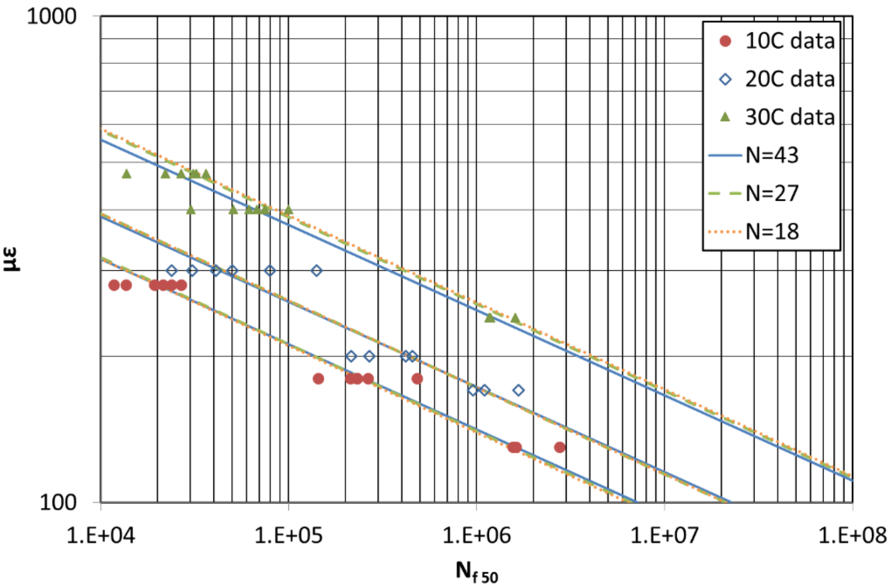

Figure 4.2: Fit of temperature dependent model to EME2 data based on different sample sizes

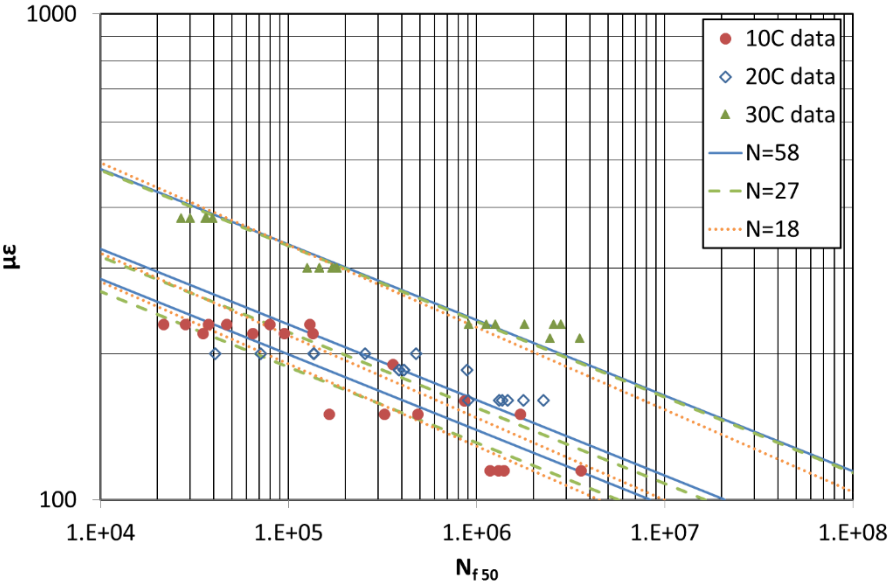

Table 4.1: Regression information reduced datasets

Mix	n	c_1	c_2	c_3	c_4	c_5	σ_y
DG20HM	43	0.4076	-10.31	84.43	-179.4	-5.705	0.3955
DG20HM	27	0.4144	-10.40	84.34	-176.9	-5.604	0.3881
DG20HM	18	0.4142	-10.40	84.44	-176.8	-5.604	0.3935
EME2	58	0.4878	-11.61	86.66	-148.1	-6.430	0.6366
EME2	27	0.4869	-11.62	86.84	-148.0	-6.428	0.5510
EME2	18	0.5221	-12.13	87.59	-142.6	-5.905	0.5790

4.2 Rest period testing

Published studies of fatigue testing including rest periods, typically consider a single load cycle followed by a specified rest period. A challenge is to configure rest periods in laboratory tests in such a way that they can be related to design situations and typical rest periods in the field. For the present study it is proposed that a different approach be taken. The intention will be to quantify the minimum benefit from healing that can be expected in the field. For the typical deep lift asphalt pavement in Queensland, a worst case scenario would be a column of B-doubles (nine axles) traversing the pavement. The typical minimum spacing between two trucks will depend on speed, but is estimated to be about 2 seconds. It is proposed that this situation be modelled in the laboratory test by nine consecutive sinusoidal load pulses, followed by a two second rest period. Figure 4.3 shows the proposed load configuration (at 10 Hz and 200 micro-strain). The results of the rest period tests will be compared to the outcomes of continuous testing to determine a healing ratio. A significant advantage of this approach is that the increase in testing time required to perform the rest period testing is ‘only’ approximately 3 times the normal test time. This compared to a single load pulse followed by a 2 second rest period, which results in a 21 times extension of testing time.

Figure 4.3: Proposed load condition in fatigue test to represent B-doubles at 2s spacing

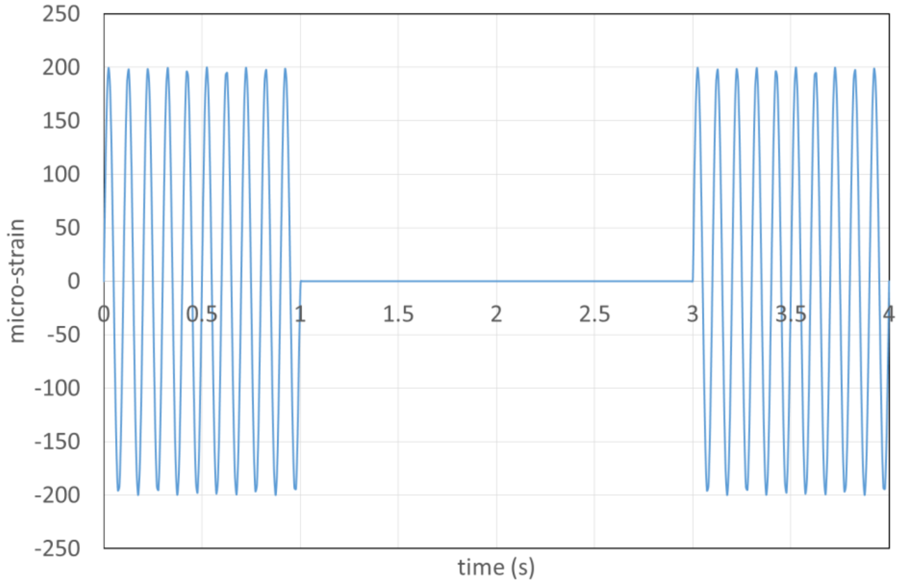

4.3 Proposed updated experimental plan

The updated laboratory testing matrix, taking into account the testing already completed in Year 2 is shown in Table 4.2. There still is sufficient material of the EME2 mix to undertake the rest period testing. Unfortunately, there is no material to perform rest period testing on the DG20HM mix. It is proposed that instead of testing 18 beams per temperature, the test matrix for testing without rest periods be reduced to 9 beams per temperature (27 beams per mix). The effect of rest periods will be assessed at 10 ˚C and 30 ˚C at the low and high strain level.

Table 4.2: Experimental plan Year 3

			Phase II (tentative)							
Asphalt mix			**DG14**		**DG14**		**DG20**		**DG20**	
Binder type			**EME2**		**A5S**		**C320**		**M1000**	
Binder content (%)			**5.6**		**tbc**		**tbc**		**tbc**	
Target air voids (%)					**5%**		**5%**		**5%**	
Temperature	Strain level	Rest period (s)	Modulus	Fatigue	Modulus	Fatigue	Modulus	Fatigue	Modulus	Fatigue
10 °C	Low	0				3		3		3
		2				3		3		3
	Medium	0			4	3	4	3	4	3
		2								
	High	0				3		3		3
		2				3		3		3
20 °C	Low	0				3		3		3
		2		3						
	Medium	0			4	3	4	3	4	3
		2								
	High	0				3		3		3
		2		3						
30 °C	Low	0				3		3		3
		2		3		3		3		3
	Medium	0			4	3	4	3	4	3
		2								
	High	0				3		3		3
		2		3		3		3		3
40 °C	N/A	N/A			4		4		4	
Total beams required			12		43		43		43	

5 INTERIM IMPLEMENTATION OPTIONS FOR DISCUSSION

This study will continue for at least another year, the work will include more laboratory experiments and the construction of field trials will also be pursued. A number of interim steps may be considered by TMR to achieve some of the benefits from this research early. Interim measures that may be considered within the existing design framework of the TMR supplement to the Austroads Guide to Pavement Technology (AGPT) include:

- Implementation of flexural modulus master curves to more accurately characterise the modulus of asphalt at elevated temperatures
- Development of mix specific fatigue curves for use in pavement design based on fatigue testing at WMAPT
- Development of mix specific, temperature dependent fatigue models for use in pavement design.

These solutions are discussed individually in the following sections. At this stage, changes to the AGPT shift factor between laboratory and field fatigue performance are not recommended, and the reasoning for this is discussed in brief.

5.1 Mix specific flexural modulus master curve

Currently, the design procedures for asphalt pavements in the AGPT are built on models that use flexural modulus to describe the load response of asphalt materials. Currently, the AGPT as well as the TMR supplement include procedures to estimate the flexural asphalt modulus at different temperatures and loading times from indirect tensile test results at 25 °C and 40ms rise time. These results are then adjusted for loading time and temperature using a standard relationship. In reality, the relationship between modulus and temperature and loading time is mix specific and better characterised using flexural modulus master curves as described in Section 2.3 of this report. It has been proposed that the flexural master curves should form the basis of design of asphalt pavements in the AGPT (Austroads 2015) and a revised text for the AGPT is currently being prepared.

It is proposed that the TMR supplement to the AGPT be updated to facilitate the development of flexural modulus master curves for Queensland mixes. This will encourage the use of asphalt mixes that have higher moduli at Queensland pavement temperatures, which may result in reduced design thicknesses.

5.2 Mix specific fatigue model at single temperature

It would be possible to provide an option in the pavement design supplement to replace the AGPT fatigue prediction function based on the Shell laboratory model shown in Equation 4, with a mix specific laboratory fatigue curve. The linear fatigue curve would be fitted in accordance with the procedures in Section 12 of this report. Since this is simply a matter of exchanging one laboratory model for another, the current reliability factor (RF) applied in the AGPT to shift laboratory results to field results could be maintained. The resulting model is provided in Equation 15.

$$N = RF \times EXP(a + b\,ln(\varepsilon)) \qquad 15$$

where

N = number of load repetitions to predicted fatigue failure in the field

RF = AGPT Reliability factor

a,b = regression coefficients

This approach would have two challenges:

1. The testing would have to be performed at the design temperature (WMAPT). This study has shown that performing flexural fatigue testing at temperatures approaching 40 °C may be challenging. Therefore, performing successful fatigue tests at the WMAPT for some urban areas in Queensland may not be possible.
2. The fatigue function is only valid for a single load frequency; 10 Hz, which according to the relationship between loading time and vehicular speed in the AGPT corresponds to 62 km/h. Using 62 km/h as a design speed may be suitable for many, but not all design situations.

The challenges can be overcome to a certain extent by making use of the relationship between modulus and loading time allowed by the master curve results. For instance, fatigue testing performed at 20 °C, 10 Hz may be converted to an equivalent modulus at 40 °C in combination with a higher frequency (higher traffic speed). However, the opportunities for temperature and loading speed adjustment are limited. It may also be argued that using a mix specific fatigue model developed from testing at 30 °C is conservative for higher design temperatures, as fatigue performance increases with the increase in temperature.

5.3 Modulus dependent model

The modulus, and therefore temperature and loading time, dependent model as presented in Section 3.2 does not have the same challenges as the single temperature model discussed in the previous section. Again it would be a matter of replacing the Shell laboratory model with a mix specific model. The AGPT shift between laboratory and field results and incorporating reliability is maintained, resulting in Equation 16.

$$N = RF \times EXP\lfloor c_1 \cdot ln^3(E) + c_2 \cdot ln^2(E) + c_3 \cdot \ln(E) + c_4 + c_5 \cdot \ln(\epsilon)\rfloor \quad 16$$

where

N = number of load repetitions to predicted fatigue failure in the field

E = flexural Modulus of the asphalt (MPa)

ε = strain in μm/m

c_1-c_5 = regression coefficients

As discussed in Section 4.1, this model could possibly be calibrated against a set of 18 fatigue specimens (6 per temperature, 2 per strain level), but for an interim implementation of this solution, it is recommended that a conservative number of 27 fatigue specimens (9 per temperature, 3 per strain level is used.

5.4 Shift between laboratory results and field performance

Currently, the AGPT uses the reliability factor (RF) to shift the predictions of the Shell laboratory fatigue model to field performance. This RF incorporates both reliability concepts and a laboratory-to-field shift factor. Both are complex factors, each made up of many components. The development of the AGPT design reliability factors was described by Jameson and Moffatt (2001).

The values of RF for asphalt pavements at different levels of desired project reliability are shown in Table 5.1.

Table 5.1: Suggested reliability factors (RF) for asphalt fatigue in AGPT (Austraods 2012)

Desired project reliability				
80%	85%	90%	95%	97.5%
2.5	2.0	1.5	1.0	0.67

5.4.1 Design reliability

It can be argued that material reliability can to a large extent be covered by selecting the desired design reliability level for the mix specific fatigue curve shown in Figure 5.1. The laboratory fatigue curve at the desired confidence level can then be used to predict field performance using a shift factor. The SPDM shift factors would not be immediately applicable though, as those were based on mean fatigue curves. Therefore, multiplying the fatigue curve at a selected level of confidence with the Shell shift factor would lead to a more conservative prediction than initially intended by Shell.

Figure 5.1: Different reliability levels for fatigue data

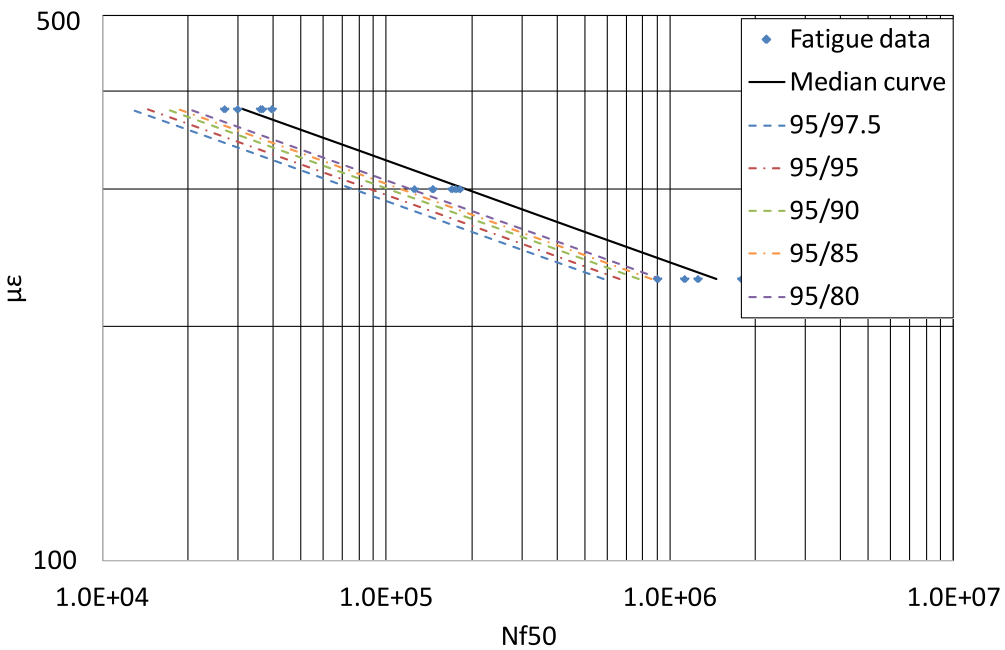

5.4.2 SPDM shift factors

The SPDM (Shell 1978) states that the fatigue data obtained in the laboratory cannot be applied directly to thickness design in the field, due to the effect of:

- random load pulse and strain distribution in the field
- intermittent loading with rest periods in between load pulses
- lateral wander of loading in the field
- healing in the asphalt
- temperature variations in the asphalt layer.

For these reasons, correction factors were introduced in the SPDM to relate the laboratory models to field performance. The effective fatigue life is taken to be a factor 2-10, higher due to the effect of healing and intermittent loading. Open graded or lean mixes would be on the low side of the range, while the high side of the range is used for dense, rich mixes. The transverse wander of the wheel loads on the pavements was considered to increase the fatigue life by a factor of about 2.5. The temperature distribution in the asphalt pavement on the other hand was considered to reduce the fatigue life by a factor of 1-3. The low range of the correction factor is relevant to low–moderate temperature regions and/or thin asphalt pavements, the higher reduction values relate to thick pavements in warm climates. The ultimate total correction factor was expected to be in the range of 10-20.

The influence of temperature and thickness on the correction factor in the SPDM was quantified more clearly in a later publication by Gerritsen and Koole (1987). The correction factors are shown in Table 5.2. In the SPDM, mixes were categorised in terms of stiffness, with S1 representing dense base courses, and S2 open graded mixes, and in terms of fatigue performance, with F1 representing mixes with moderate bitumen and air void content and F2 mixes with high air void content. The values in the table show the influence of temperature on expected fatigue life to be greater for thin asphalt pavements than for thick pavements. Stiff mixes, at low temperatures are expected to have a low fatigue life. The values in Table 5.2 were used in the development of the design charts in the SPDM.

Table 5.2: Factors correcting for the combination of intermittent loading, lateral distribution of wheel loads and temperature gradients in the asphalt layer

Thickness of asphalt layer	wMAAT	Mix code			
mm	°C	S1-F1	S2-F1	S1-F2	S2-F2
h_1<100	4	15	15	10	5
	12	20	20	15	10
	20	20	20	15	10
	28	25	25	20	15
100<h_1<200	4	15	15	10	5
	12	15	15	10	10
	20	15	15	15	10
	28	15	15	15	10
h_1>200	4	10	10	10	5
	12	10	10	10	5
	20	10	10	10	5
	28	10	10	10	5

Source: Gerritsen and Koole (1987)

If fatigue results and modulus are compared for DG20C600 at 20 °C to chart M-3 in the design manual, this mix is best described as an F1 within the Shell pavement design framework. The modulus characteristics of the mix further class it as an S1 using Chart M-2.

Since it is unlikely that an open graded asphalt will be used in a structural layers by TMR, materials used in these layers will without exception be expected to fall within the S2 category. From Table 5.2 it can be appreciated that the value of the correction factor proposed by Shell would never be less than 10 for structural layers in Queensland.

5.4.3 Discussion on shift factor

It should be clear from the above discussion that the shift of mean fatigue curves from laboratory to field by means of the factor RF as currently applied in the AGPT will lead to more conservative fatigue prediction results than applying the shift factor in the order of 10 applied by Shell. However, in view of the lack of local field calibration data, changes to the RF are not recommended for consideration at this stage, unless, TMR is willing to consider using a shift factor of 10 in combination with the desired level of design reliability in the fatigue test.

An alternative approach would be to make the RF a function of temperature. Based on the laboratory fatigue results obtained at high temperatures, a higher value for RF may be proposed for design temperatures above 20 °C.

5.5 Design example

To demonstrate the possible impact of interim solutions on design thicknesses, the different interim solutions for consideration are used in a design example. The modulus and fatigue data for the DG20HM and EME2 mixes obtained as part of this study are used in the example. The thickness design will be for a full depth asphalt pavement on a subgrade with a stiffness of 70 MPa. The design is for a pavement carrying 100 million standard 80 kN dual wheel axles, with a tyre inflation pressure of 750 kPa. The WAMPT is 32 °C and the design traffic speed is 60 km/h. The desired project reliability is 95%. The influence of the surfacing layer is ignored in this example.

Different design options are considered, which are summarised in Table 5.3. The table also provides references to the relevant input data for the design models in tables elsewhere in this report. The base case (Option 1) is to perform the design using the current AGPT approach. ITT results for the EME2 and DG20HM mixes were determined for this purpose. The average of three resilient modulus for the DG20HM at 25 °C, 40ms rise time is 4641 MPa, whereas the average resilient modulus for the EME2 under the same conditions is 8317 MPa. The resilient modulus values are corrected for the WMAPT and traffic speed using the procedures in AGPT. Option 2 considers the use of the flexural master curve instead of the ITT relationships. Option 3 introduces the use of a mix specific fatigue model developed for a single temperature, whereas the temperature dependent fatigue functions are used as part of Option 4. Option 5 finally combines the 95/95 confidence limit temperature dependent fatigue curve with the lower limit of the Shell shift factor (10).

Table 5.3: Summary of design options

Option	Modulus determination	Fatigue model	Shift factor
1	ITT corrected for WMAPT and speed	AGPT (Table 3.2)	1.0
2	Flexural master curve (Table 2.1)	AGPT (Table 3.2)	1.0
3	Flexural master curve (Table 2.1)	Mix specific linear (Table 3.1)	1.0
4	Flexural master curve (Table 2.1)	Mix specific temperature dependent (Table 3.3)	1.0
5	Flexural master curve (Table 2.1)	Mix specific temperature dependent 95/95 confidence level (Table 3.3)	10

The modulus information for the pavement materials under the different options is provided in Table 5.4.

Table 5.4: Pavement material modulus information

Option	DG20HM	EME2	Subgrade
1	2249	4030	70
2,3,4,5	1986	4621	70

Thickness designs were compared using multitudes of 25 mm. The first thickness to yield a fatigue prediction in excess of 1E8 was selected as the design thickness. The results are shown in Table 5.5. It should be noted that the subgrade limiting strain criterion was checked for all design cases. For each of the cases the number of load repetitions to failure is larger for this parameter than the asphalt fatigue life.

Table 5.5: Results

Option	Mix	Design thickness (mm)	Load repetitions
1	DG20HM	350	1.44E8
1	EME2	275	1.44E8
2	DG20HM	350	1.14E8
2	EME2	275	1.89E8
3	DG20HM	325	1.06E8
3	EME2	225	3.09E8
4	DG20HM	350	1.21E8
4	EME2	225	1.78E8
5	DG20HM	300	1.43E8
5	EME2	200	1.72E8

The results in Table 5.5 indicate the following for the mixes under study:

- Changing the method of modulus characterisation from the ITT to the flexural modulus master curve did not change the design thickness, although the number of load repetitions to failure for the EME2 mix did increase.
- Using the single temperature linear fatigue model lead to a reduction in the design thickness of 25 mm for the DG20HM mix and 50 mm for the EME2 mix
- Using the temperature dependent fatigue model resulted in a reduction of 50 mm for the EME2 mix, but no reduction for the DG20HM mix
- Using the 95/95 confidence limit for the temperature dependent model in combination with the shift factor of 10 resulted in a reduction of 50 mm for the DG20HM and 75 mm for the EME2 mix.

As expected, the relative change in thickness will depend on how well the Shell laboratory fatigue prediction model compares to the mix specific fatigue results.

6 CONCLUSIONS AND RECOMMENDATIONS

The object of Year 2 of the study was to characterise the fatigue performance of typical Queensland asphalt mixes at elevated temperatures. The study also explored the effects of healing and rest periods and evidence of a fatigue endurance limit in the test.

A further aim was to propose initial improved models for the prediction of fatigue in asphalt pavements in Queensland. An assessment was performed to evaluate to what extent these models will lead to reduced pavement thicknesses.

The findings of the study indicate that the fatigue performance of asphalt mixes can be successfully characterised using the new AGPT/T274 protocol up to temperatures of at least 30 °C. It was found that at a temperature of 40 °C, the test equipment was no longer able to impart a well-controlled sinusoidal-shaped displacement loading on the sample.

The results of the study show the benefits of developing mix-specific fatigue curves. The Shell laboratory model was developed based on the average results of twelve mixes and as such provides a good estimate for the fatigue behaviour of some mixes, but not of others, especially at elevated temperatures.

It appears to be possible to obtain a good statistical fit for a temperature-dependent regression model based on the results for 18 beam specimens divided over three temperatures. Further work will be done to confirm this, for the moment it is proposed that 27 beams be tested to characterise mix fatigue performance at different temperatures.

A number of options for interim improvements to the asphalt pavement design methods used by TMR were listed in this study. Consultation with the Department will take place to discuss implementation. More data on the fatigue performance of Queensland mixes is required to finalise the models.

The introduction of the option to develop mix specific fatigue functions for use in pavement design may be expected to drive three outcomes:

1. Optimisation of mixes in terms of balancing rut resistance, stiffness and fatigue performance
2. Encouragement of the use of innovative asphalt mix designs (e.g. EME2)
3. A significant reduction in pavement thicknesses.

A methodology to characterise fatigue performance at different temperatures was developed under this study. This will be used to characterise more typical Queensland asphalt mixes in Year 3. The focus will now shift to capturing the effect of rest periods and healing on fatigue performance.

REFERENCES

Austroads 2012, *Guide to pavement technology*: *part 2: pavement structural design*, 3rd edn, Austroads Sydney, NSW.

Austroads 2014, *High modulus high fatigue asphalt (EME2) technology transfer,* by L Petho J Griffin, A Beecroft & E Denneman, AP-T283-14, Austroads, Sydney, NSW.

Austroads 2015, *Improved design procedures for asphalt pavements: outcomes for year 2 of 3,* by E Denneman, A Beecroft, D Bodin & J Griffin, AP-T296-15, Austroads, Sydney, NSW.

Bazin, P & Saunier, J 1967, 'Deformability, fatigue and healing properties of asphalt mixes', *Proceedings: second international conference on the structural design of asphalt pavements*, *Ann Arbor*, *Michigan*, International Society for Asphalt Pavements, Lino Lakes, MN, USA, pp. 553-69.

CROW 2010, *Publicatie 285: asfalt in weg- en waterbouw* (in Dutch), CROW, Ede, Netherlands.

Gerritsen, A & Koole, R 1987, 'Seven years' experience with the structural aspects of the Shell Pavement Design Manual', *Proceedings of the sixth international conference on structural design of asphalt pavements: volume 1*, University of Michigan, Ann Arbor, Michigan, USA, pp. 94-106.

Jameson, G & Moffatt, M 2001, 'Development of Austroads pavement design reliability guidelines', APRG 00/17, ARRB Group, Vermont South, Vic.

Mateos, A, Ayuso, J, Cadavid, B, & Marron, J 2012, 'Lessons learned from the application of the CalME asphalt fatigue model to experimental data from CEDEX test track', in Jones, D, Harvey, J, Mateos, A & Al-Qadi, IL (eds), *Advances in pavement design through full scale accelerated pavement testing,* CRC Press, Boca Raton, Florida, USA, pp. 483-92.

NACoE, forthcoming a 'Asphalt fatigue at Queensland temperatures: literature review and experiment design', contract report for Queensland Department of Transport and Main Roads, ARRB Group, Albion QLD

NACoE, forthcoming b, 'Cost effective design of thick asphalt pavements: high modulus asphalt implementation', contract report for Queensland Department of Transport and Main Roads, ARRB Group, Vermont South, Vic

Pellinen, T, Christensen, D, Rowe, G & Sharrock, M 2004, 'Fatigue-transfer functions: how do they compare?' *Transportation Research Record*, no. 1896, pp. 77-87.

Shell 1998, *SPDM 3.0*, software, Shell International Oil Product, Amsterdam, Netherlands.

Shell International Petroleum 1978, *Pavement design manual: asphalt pavement and overlays for road traffic*, Shell International Petroleum Company, London, UK.

Stuart, K, Mogawer, W & Romero, P 2002, *Validation of the Superpave asphalt binder fatigue cracking parameter using an accelerated loading facility,* FHWA-RD-01-093, Federal Highway Administration, McLean, Virginia, USA.

Tsai, B-W 2003, *High temperature fatigue and fatigue damage process of aggregate-asphalt mixes*, University of California at Berkeley, Institute of Transportation Studies, Pavement Research Center, Richmond, CA, USA.

Van Dijk, W & Visser, W 1977, ‘Energy approach to fatigue for pavement design’, *Asphalt Paving Technology*, vol. 46, pp. 1-39.

Witczak, M, Mamlouk, M, Souliman, M & Zeiada, W 2013*, Laboratory validation of endurance limit for asphalt pavements*, NCHRP report 762, Transportation Research Board, Washington, DC, USA.

APPENDIX A EXPERIMENTAL DATA

Table A 1: Flexural modulus results DG20 C600

Temperature (°C)	Frequency (Hz)	Flexural modulus for replicate specimens (MPa)				Statistics		
		148-2	148-3	149-1	149-3	Mean	STDEV	CoV
5	0.1	9,884	11,028	10,841	10,046	10565	556	5.3%
	0.5	12,376	13,736		12,516	13091	747	5.7%
	1	13,337	14,926	14,268	13,460	14183	766	5.4%
	3	14,915	16,863	15,914	15,096	15930	931	5.8%
	5	15,758	17,885	16,461	15,924	16783	1039	6.2%
	10	17,073	19,003	17,462	16,705	17849	1087	6.1%
	15	17,181	19,917	18,394	17,259	18534	1351	7.3%
	20	17,559	21,052	18,795	18,090	10565	556	5.3%
10	0.1	4,489	5,020	5,022	4,852	4881	231	4.7%
	0.5	6,429	7,067	7,085		6912	322	4.7%
	1	7,411	8,124	7,962	7,823	7889	295	3.7%
	3	9,022	9,870	9,577	9,389	9546	357	3.7%
	5	9,880	10,769	10,489	10,026	10387	415	4.0%
	10	10,848	12,084	11,414	11,065	11499	571	5.0%
	15	11,405	12,743	11,991	12,081	12193	566	4.6%
	20	11,806	13,325	12,273	12,363	12618	679	5.4%
20	0.1	1,680	1,593	1,406	1,346	1524	141	9.3%
	0.5	2,801		2,501	2,358	2553	226	8.9%
	1	3,485	3,379	3,134	2,898	3255	238	7.3%
	3	4,735	4,602	4,360	3,995	4459	292	6.6%
	5	5,422	5,256	5,001	4,618	5111	314	6.1%
	10	6,283	6,315	5,839	5,498	6050	369	6.1%
	15	6,834	6,752	6,441	5,972	6550	356	5.4%
	20	7,222	7,089	6,736	6,234	6874	401	5.8%
30	0.1	595	577	577	528	571	25	4.4%
	0.5			938	931	935	5	0.5%
	1	1,255	1,255	1,225	1,172	1232	36	2.9%
	3	1,830	1,913	1,820	1,721	1839	80	4.3%
	5	2,157	2,233	2,172	2,001	2159	95	4.4%
	10	2,696	2,861	2,742	2,539	2740	134	4.9%
	15	3,065	3,147	3,048	2,844	3050	124	4.1%
	20	3,286	3,381	3,225	3,027	3260	146	4.5%
40	0.1	299	304	293	190	278	49	17.8%
	0.5	423	393	428	333	394	38	9.6%
	1	524	503	565	424	504	51	10.2%
	3	762	764	835	642	753	70	9.2%
	5	917	869	975	778	882	73	8.2%

Temperature (°C)	Frequency (Hz)	Flexural modulus for replicate specimens (MPa)				Statistics		
		148-2	148-3	149-1	149-3	Mean	STDEV	CoV
	10	1169	1193	1257	998	1162	97	8.4%
	15	1305	1331	1346	1136	1290	87	6.8%
	20	1421	1441	1534	1223	1412	114	8.1%
	0.1	299	304	293	190	278	49	17.8%

Figure A 1: Linear regression plot DG20HM at 10 °C

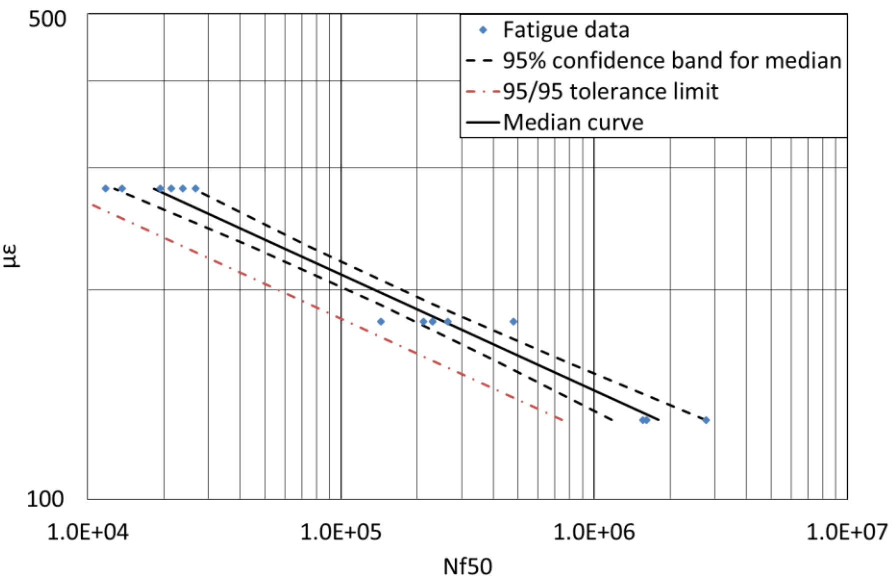

Figure A 2: Linear regression plot DG20HM at 20 °C

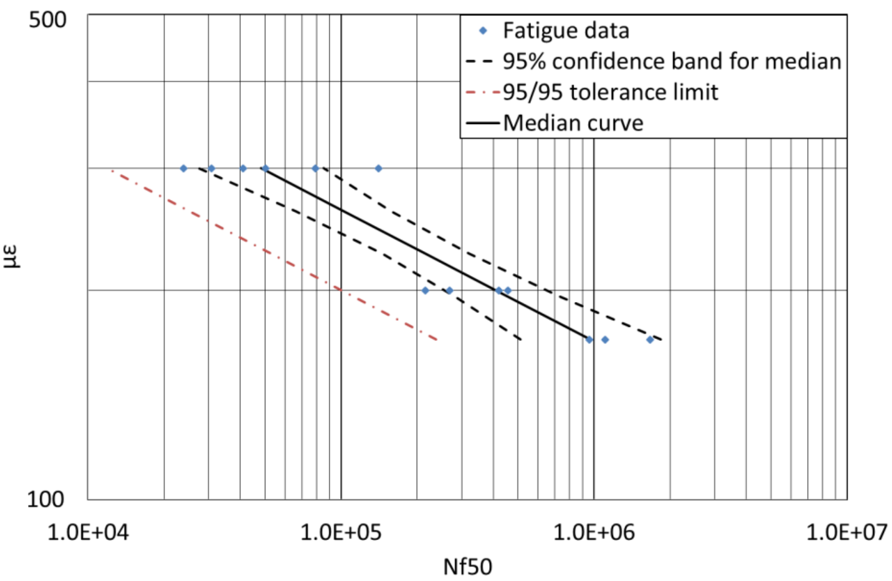

Figure A 3: Linear regression plot DG20HM at 30 °C

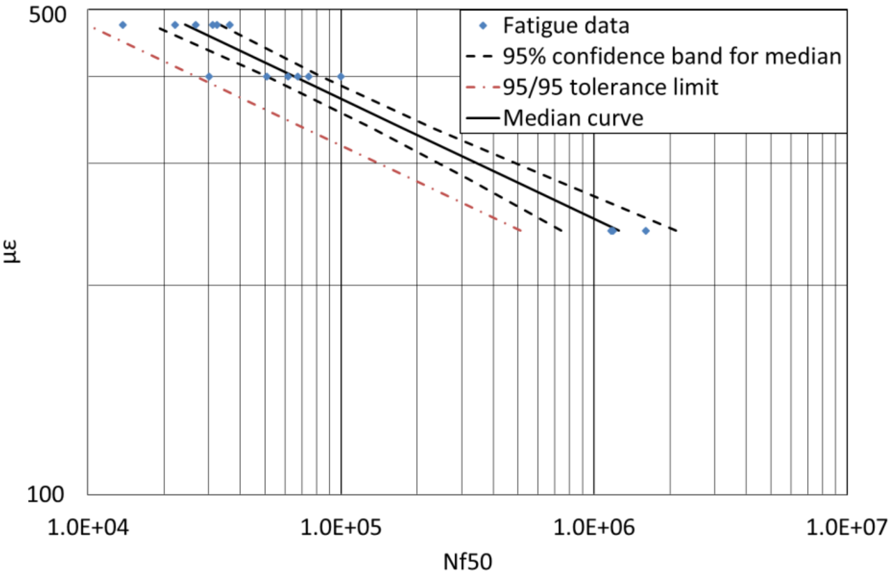

Figure A 4: Linear regression plot EME2 at 10 °C

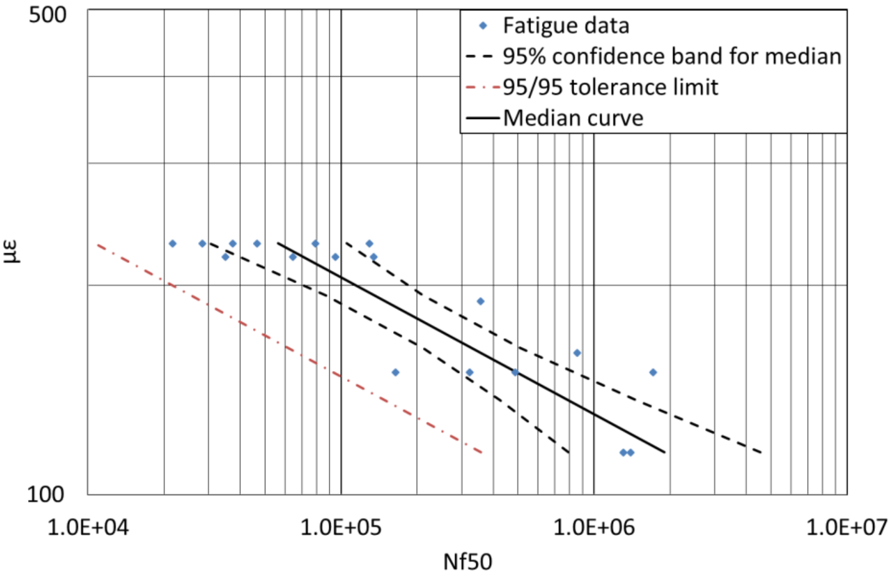

Figure A 5: Linear regression plot EME2 at 20 °C

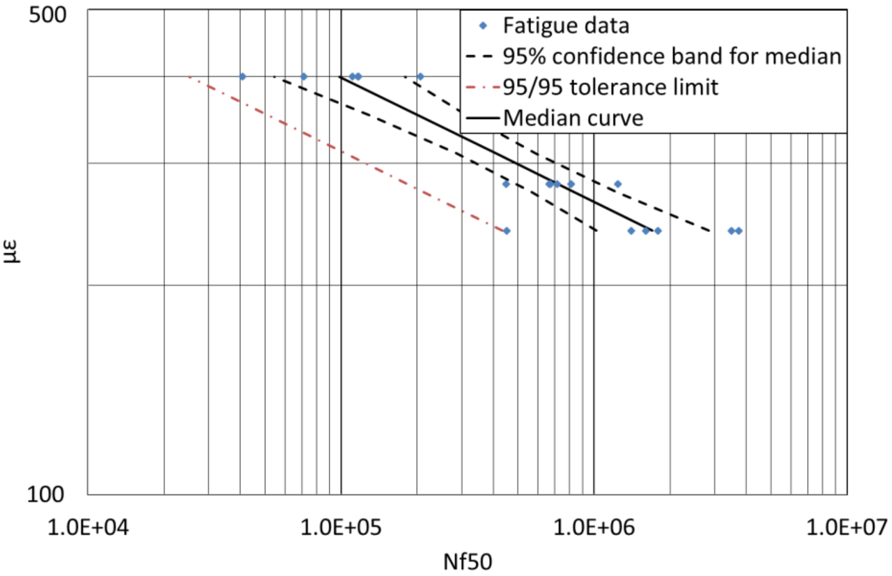

Figure A 6: Linear regression plot EME2 at 30 °C